GlueX Photon Source Characteristics as a Function of Electron Beam Energy

R.T. Jones

November 12, 2004

Abstract

The GlueX Design Report contains a detailed description of the characteristics of the photon source assuming an electron beam energy of 12 GeV. The purpose of this note is to explore how these characteristics change as the electron beam energy is varied. This is a supplement to the information contained in the design report, and does not represent any updates in the basic design of the source presented there.

The final table in chapter 4 of the GlueX Design report v4 is reproduced as Table 1 below. All four columns of numbers were obtained for the same beam conditions, except that the crystal orientation was adjusted to align the coherent intensity peak at the energy listed in row one. The second row, labeled N_γ, gives the integrated rate of beam photons in the coherent peak downstream of the collimator. Note the sharp decrease in the intensity of the coherent peak as the energy approaches the end point. By contrast, the incoherent bremsstrahlung flux is approximately constant over this range of energies. The third and fourth row show the height and width of the peak in the polarization spectrum of the beam. Rows five and six report the height and width of the peak in the tagging efficiency spectrum. The tagging efficiency is defined as the number of beam photons of a particular energy reaching the target divided by the corresponding rate in the tagging focal plane. Large tagging efficiencies are required in order to make effective use of tagging. The width of the peak in the tagging efficiency spectrum determines the width of the focal plane that would be active when running with collimation. The peak integral reported in row two is summed within the

Table 1: Operating parameters for an experiment using the coherent bremsstrahlung beam. The calculation assumes a 12 GeV electron beam energy and a 3.4 mm collimator 80 m downstream from a radiator of thickness 10^{-4} radiation lengths. The electron beam current is taken to be 3 μA. The rates in the detector (last two rows) are calculated for a 30 cm liquid hydrogen target and an open hadronic trigger.

E of peak	8 GeV	9 GeV	10 GeV	11 GeV
N_γ in peak	185 M/s	100 M/s	45 M/s	15 M/s
peak polarization	0.54	0.41	0.27	0.11
(f.w.h.m.)	(1140 MeV)	(900 MeV)	(600 MeV)	(240 MeV)
peak tagging efficiency	0.55	0.50	0.45	0.29
(f.w.h.m.)	(720 MeV)	(600 MeV)	(420 MeV)	(300 MeV)
power on collimator	5.3 W	4.7 W	4.2 W	3.8 W
power on target	810 mW	690 mW	600 mW	540 mW
total hadronic rate	385 K/s	365 K/s	350 K/s	345 K/s
tagged hadronic rate	26 K/s	14 K/s	6.3 K/s	2.1 K/s

f.w.h.m. tagging efficiency window. Rows seven and eight give the photon beam power that is incident on the experimental target (and photon beam dump) and the photon collimator, respectively.

The last two rows in Table 1 give the inclusive and tagged rates for hadronic triggers from a 30 cm liquid hydrogen target placed in the beam following the collimator. Note that the total hadronic rate is dominated by background (*i.e.* non-tagged) events associated with the low-energy component of the beam. This is why the total trigger rate is essentially constant while the flux in the coherent peak varies with peak energy over an order of magnitude. This table illustrates the value of having an electron beam energy well above the photon energy needed for the experiment.

The above comparison is obtained by keeping the electron beam parameters fixed and simply rocking the crystal. There were two factors which were considered in deciding what the limits of the tagged window should be: the polarization, and the tagging efficiency. Both factors peak at the coherent edge and decrease with decreasing photon energy. Of the two, the tagging efficiency is the more steep function, so it was used to limit the size of the tagged window. For the study of the dependence of the source parameters on the electron beam energy, the F.W.H.M. of the tagging efficiency listed

Table 2: Operating parameters for the GlueX photon source under conditions of varying electron beam energy. The collimator distance and diameter are kept constant at 80 m and 3.4 mm, respectively, and the radiator thickness is 10^{-4} radiation lengths. be 3 μA. The rates in the detector (last two rows) are calculated for a 30 cm liquid hydrogen target and an open hadronic trigger.

electron beam energy	10 GeV	11 GeV	12 GeV	13 GeV
electron beam current	4.3 μA	3.5 μA	3.0 μA	2.5 μA
N_γ in peak	32 M/s	67 M/s	100 M/s	130 M/s
peak polarization	0.14	0.28	0.41	0.48
average polarization	0.08	0.24	0.37	0.47
peak tagging efficiency	0.25	0.43	0.50	0.57
average tagging efficiency	0.15	0.29	0.41	0.51
power on collimator	4.4 W	4.4 W	4.5 W	4.5 W
power on target	510 mW	610 mW	730 mW	850 mW
total hadronic rate	370 K/s	370 K/s	370 K/s	370 K/s
tagged hadronic rate	5 K/s	10 K/s	16 K/s	21 K/s

in the second column of Table 1 has been used to set the tagging window to the range 8.4 - 9.0 GeV. To facilitate the comparison between collimated and uncollimated beams, the electron beam current was adjusted to maintain a constant total hadronic rate in the target of 370 KHz.

Numerical results are shown in Table 2. The same results are shown graphically in Figs. 1-4 for polarization and Figs. 5-8 for flux. Figs. 1,5 show that at the large-angle setting chosen for the 10 GeV end-point case there is an extra peak at 8.4 GeV that appears. This comes from the accidental overlap of the desired reciprocal lattice vector of the crystal with another higher-order vector from another region of q-space. The polarization in this peak lies in a different plane from the primary peak at 9 GeV, so under actual operating conditions it would be desirable to adjust one of the goniometer angles to rotate it away. This is possible to do, in general, without affecting the alignment of the primary edge. This peak actually appears in the other spectra as well, but at energies above the primary peak where it is interspersed among the higher-order recurrences of the primary peak. Its presence does not affect the results shown, so no effort was made to eliminate it for the purposes of this study.

An overall figure of merit for the combination of flux enhancement and

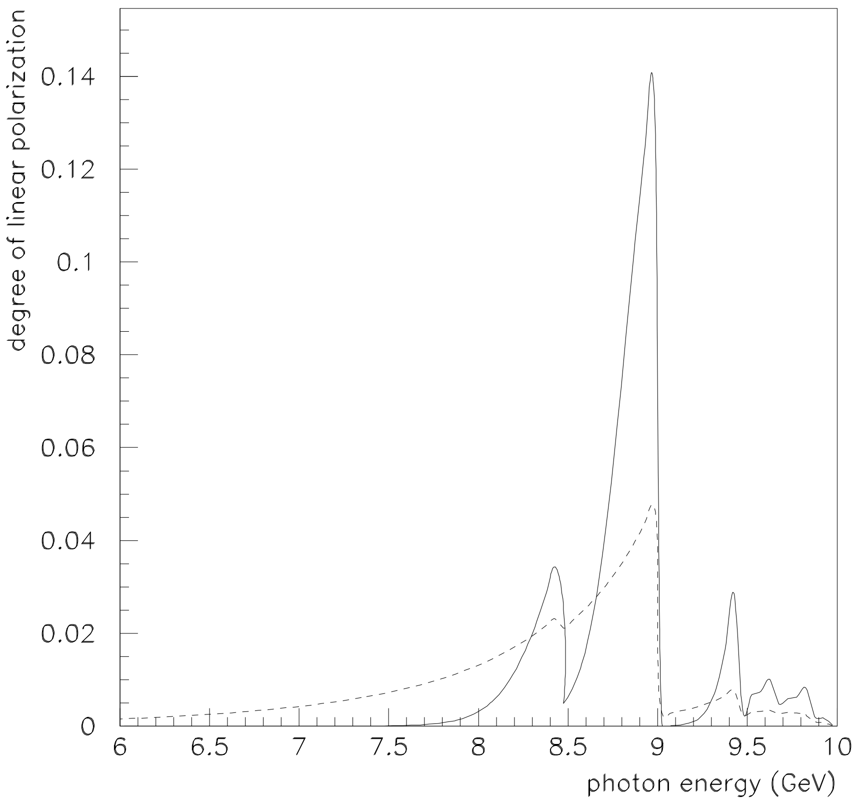

Figure 1: Degree of linear polarization *vs* photon energy for the GlueX coherent bremsstrahlung source for a 10 GeV electron beam, with collimation (solid curve) and without (dashed curve).

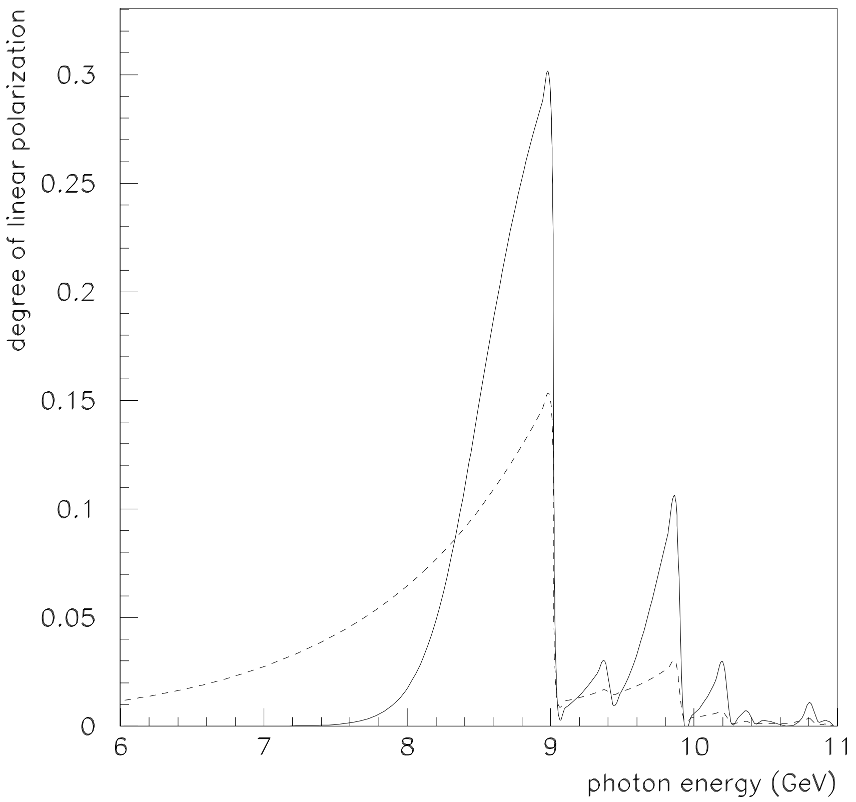

Figure 2: Degree of linear polarization *vs* photon energy for the GlueX coherent bremsstrahlung source for a 11 GeV electron beam, with collimation (solid curve) and without (dashed curve).

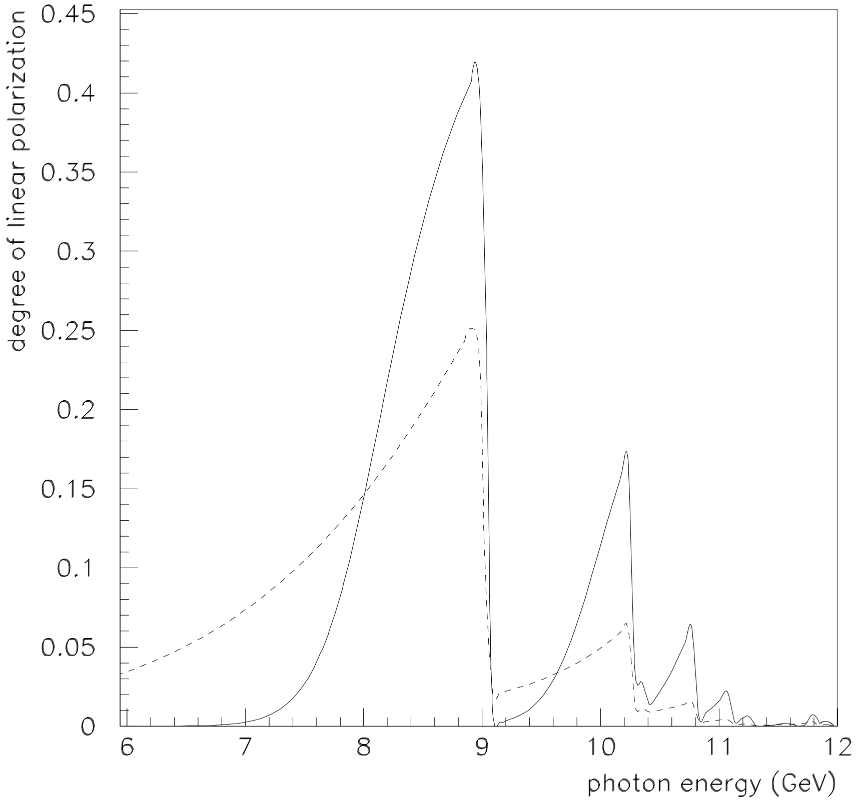

Figure 3: Degree of linear polarization *vs* photon energy for the GlueX coherent bremsstrahlung source for a 12 GeV electron beam, with collimation (solid curve) and without (dashed curve).

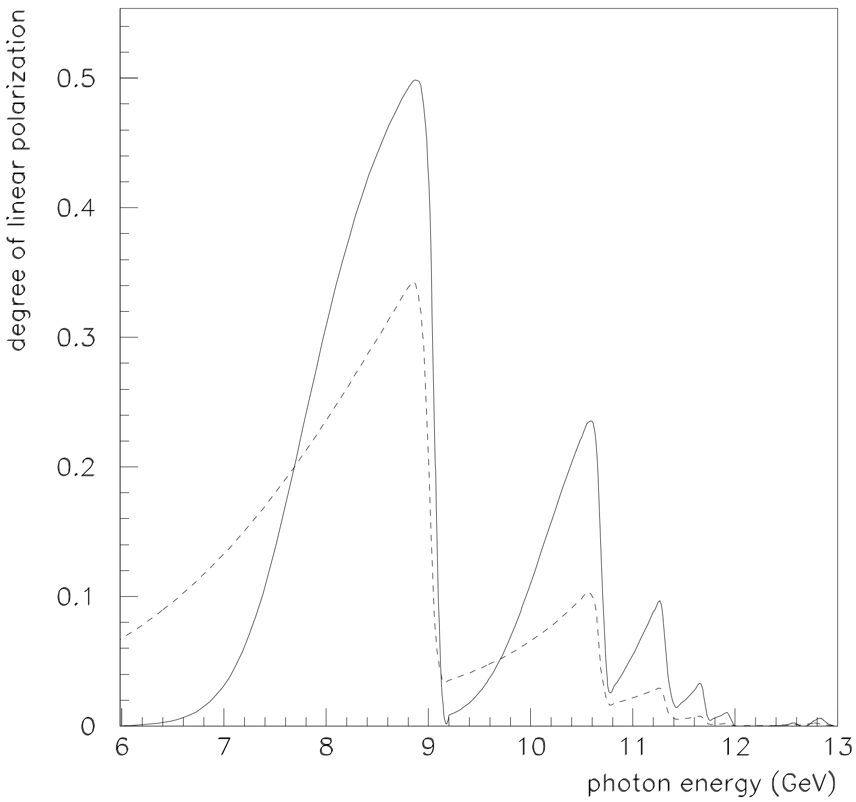

Figure 4: Degree of linear polarization *vs* photon energy for the GlueX coherent bremsstrahlung source for a 13 GeV electron beam, with collimation (solid curve) and without (dashed curve).

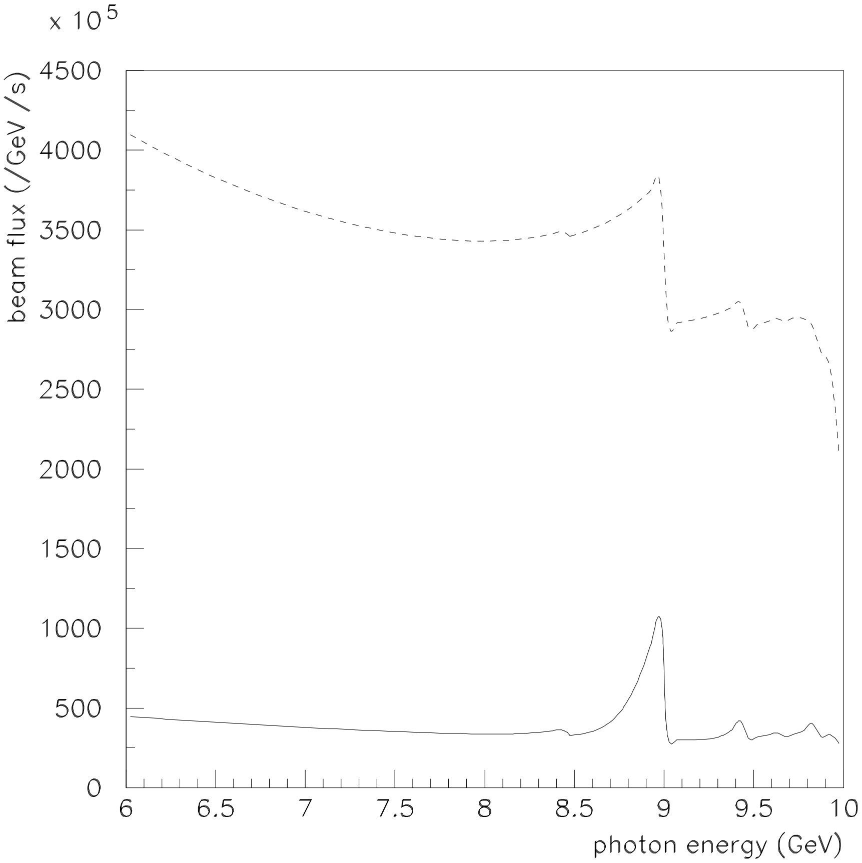

Figure 5: Photon beam rates *vs* photon energy for the GlueX coherent bremsstrahlung source for a 10 GeV electron beam, with collimation (solid curve) and without (dashed curve). Rates are normalized as shown in Table 2.

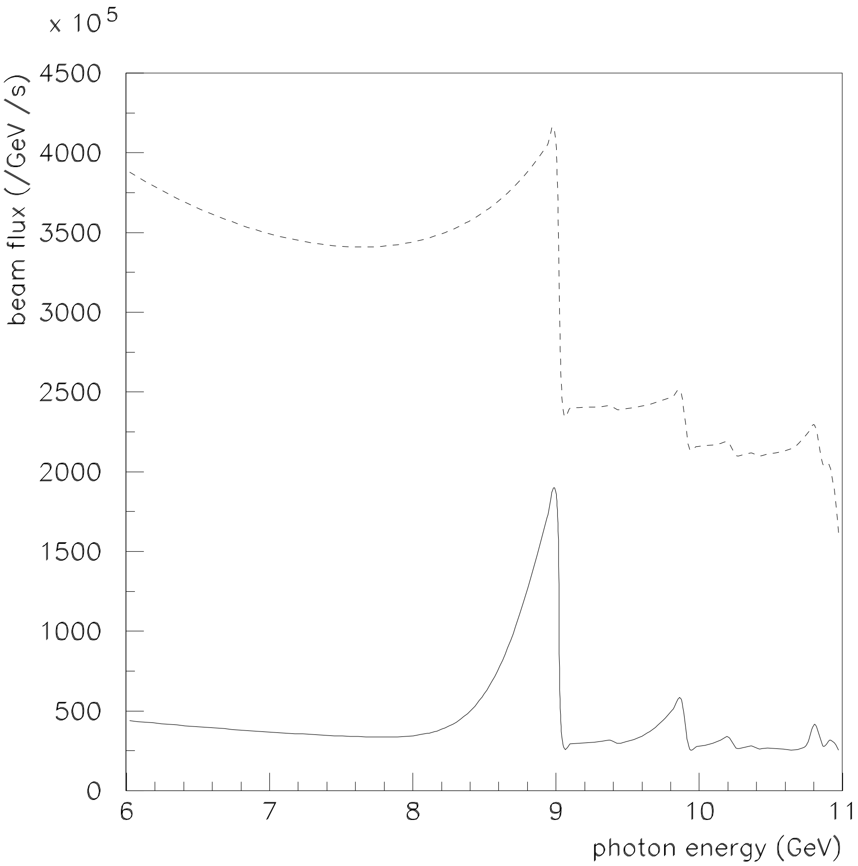

Figure 6: Photon beam rates *vs* photon energy for the GlueX coherent bremsstrahlung source for a 11 GeV electron beam, with collimation (solid curve) and without (dashed curve). Rates are normalized as shown in Table 2.

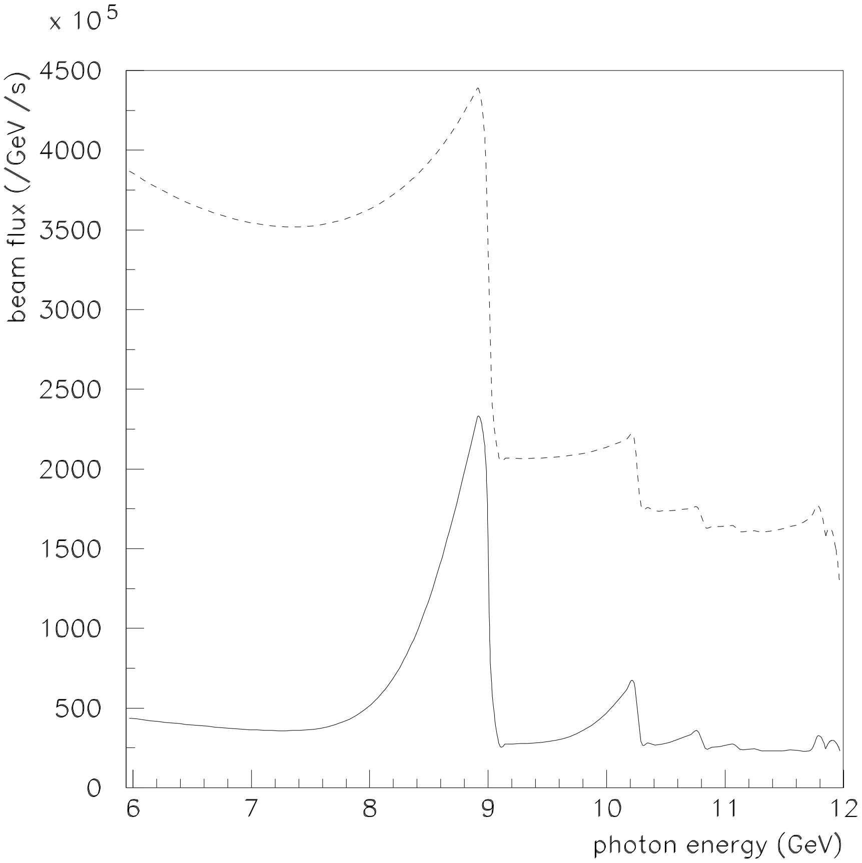

Figure 7: Photon beam rates *vs* photon energy for the GlueX coherent bremsstrahlung source for a 12 GeV electron beam, with collimation (solid curve) and without (dashed curve). Rates are normalized as shown in Table 2.

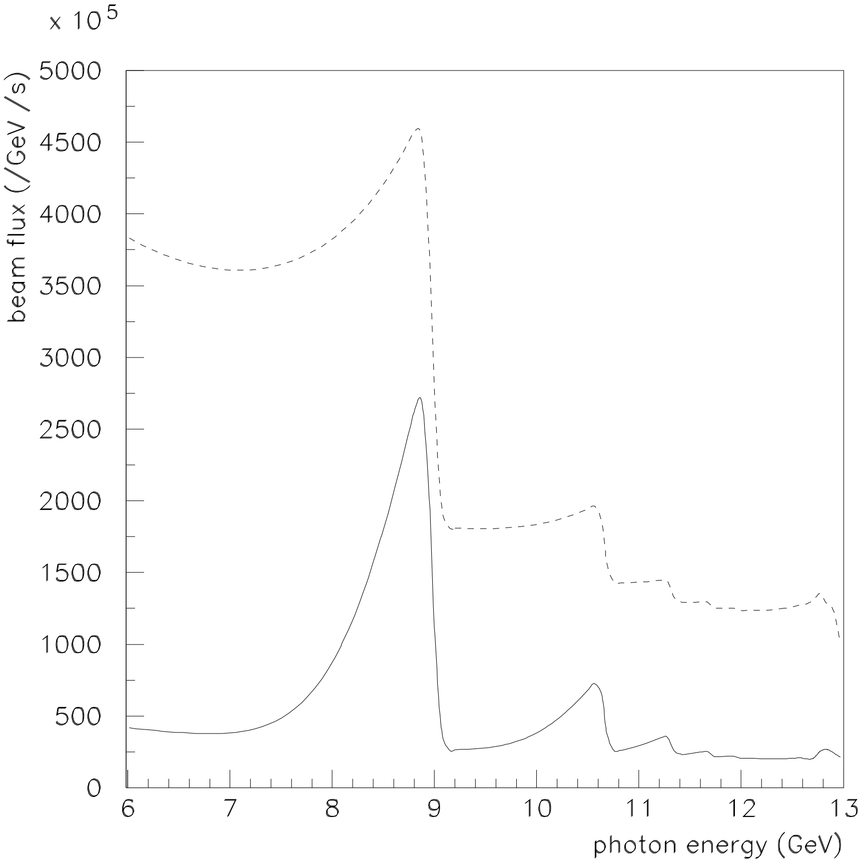

Figure 8: Photon beam rates *vs* photon energy for the GlueX coherent bremsstrahlung source for a 13 GeV electron beam, with collimation (solid curve) and without (dashed curve). Rates are normalized as shown in Table 2.

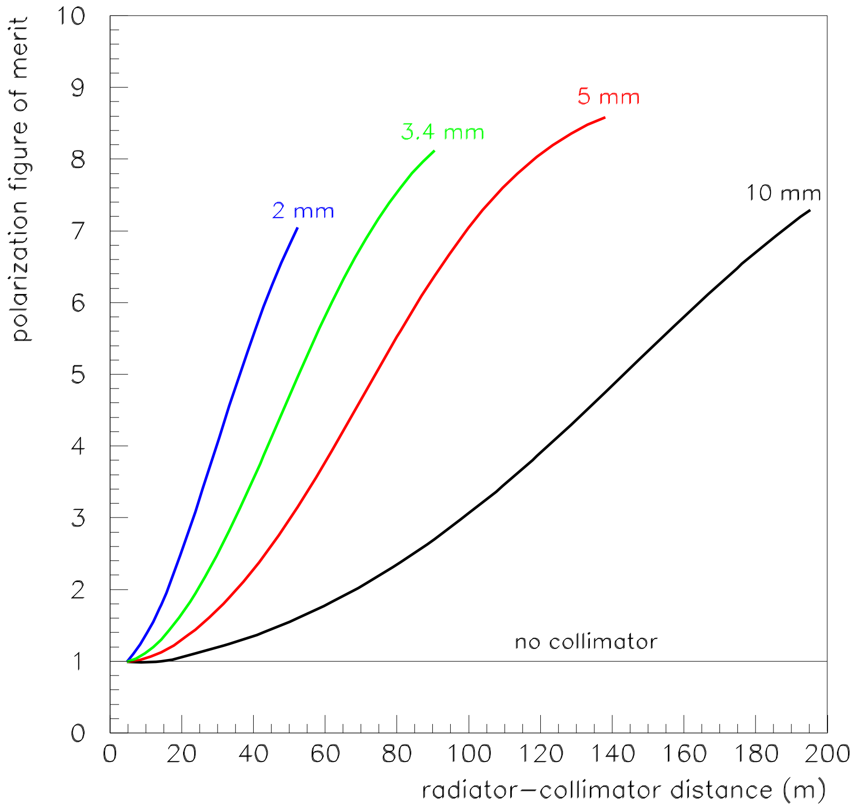

Figure 9: Photon beam figure of merit, defined by Eq. 1, plotted as a function of the radiator-collimator distance, for a variety of collimator apertures (colored curves) and for no collimator (black curve). The vertical scale is defined by setting the FOM for the uncollimated case to unity.

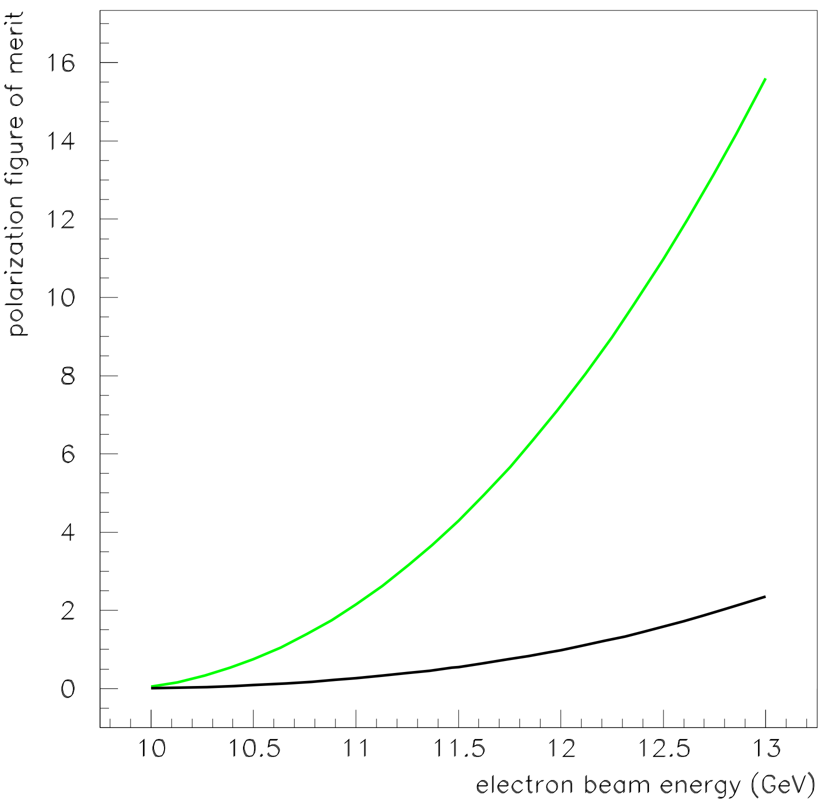

Figure 10: Photon beam figure of merit, defined by Eq. 1, plotted as a function of the electron beam energy, under conditions of constant total hadronic background rates in the detector. The green curve is for a 3.4 mm collimator at 80 m from the radiator, and the black curve is for an uncollimated beam.

polarization for the GlueX photon source is defined by Eq. 1.

$$\mathrm{FOM} = P^2 F \tag{1}$$

where P is the degree of linear polarization averaged over the tagged window, and F is the total photon flux on target within the same window. Thus defined, the FOM is a relative measure of the sensitivity of an experiment to a small signal in a polarization observable. The overall scale for the beam flux factor F is determined by the maximum beam intensity at which the detector can operate effectively. The GlueX it is expected that the first-level trigger rate will be the limiting factor in setting the beam current. The first-level trigger rate is determined by the total hadronic rate in the target. Therefore the FOM is defined as the product of mean-squared polarization in the tagged peak and the flux at fixed total hadronic rate in the detector, which was chosen to be 370 KHz, as shown in Table 2.

In Fig. 9 is shown the dependence of the FOM on the distance between the radiator and collimator, under constant electron beam conditions and hadronic background rates in the detector. The limit of a large collimator aperture is shown by the black line as a normalization reference. In Fig. 10 is shown the dependence of the FOM on the electron beam energy, under constant conditions of collimation and hadronic background rates in the detector. All electron beam properties (emittance, spot size, energy resolution) were held constant in this study, as the beam energy was varied.

One concern that is not explicit in the FOM is the tagging efficiency, which determines the effectiveness of the tagging coincidence for determining the photon energy for any given event. The tagging efficiency is implicitly incorporated into this analysis by its role in setting the size of the window of tagged photons which is subtended by the active tagging counters. It also played a role in the choice of the collimator diameter, by limiting the extent to which further collimation can be exploited to improve polarization and flux conditions for the beam. This is why the curves for 2 mm, 3.4 mm, and 5 mm collimators cannot be extended indefinitely in Fig. 9. For the purposes of this figure, the curves terminate at the point where the peak tagging efficiency drops below 30%.